

Synthesis, Structure, and Reactivity of Ru^{II} Complexes with Trimethylsilylethynylamidinate Ligands

Wolfram W. Seidel,^[a] Woldemar Dachtler,^[a] and Tania Pape^[b]

Keywords: N-ligands; Metathesis; Chelates; Substituent effects; X-ray diffraction

Abstract. The mononuclear amidinate complexes $[(\eta^6\text{-cymene})\text{RuCl}(\mathbf{1a})]$ (**2**) and $[(\eta^6\text{-C}_6\text{H}_6)\text{RuCl}(\mathbf{1b})]$ (**3**), with the trimethylsilyl-ethynylamidinate ligands $[\text{Me}_3\text{SiC}\equiv\text{CC}(\text{N}-c\text{-C}_6\text{H}_{11})_2]^-$ (**1a**⁻) and $[\text{Me}_3\text{SiC}\equiv\text{CC}(\text{N}-i\text{-C}_3\text{H}_7)_2]^-$ (**1b**⁻) were synthesized in high yields by salt metathesis. In addition, the related phosphane complexes $[(\eta^5\text{-C}_5\text{H}_5)\text{Ru}(\text{PPh}_3)(\mathbf{1b})]$ (**4a**) $[(\eta^5\text{-C}_5\text{Me}_5)\text{Ru}(\text{PPh}_3)(\mathbf{1b})]$ (**4b**), and $[(\eta^6\text{-C}_6\text{H}_6)\text{Ru}(\text{PPh}_3)(\mathbf{1b})](\text{BF}_4)$ (**5-BF**₄) were prepared by ligand ex-

change reactions. Investigations on the removal of the trimethyl-silyl group using $[\text{Bu}_4\text{N}]F$ resulted in the isolation of $[(\eta^6\text{-C}_6\text{H}_6)\text{Ru}(\text{PPh}_3)\{(\text{N}-i\text{-C}_3\text{H}_7)_2\text{CC}\equiv\text{CH}\}](\text{BF}_4)$ (**6-BF**₄) bearing a terminal alkynyl hydrogen atom, while **2** and **3** revealed to yield intricate reaction mixtures. Compounds **1a/b** to **6-BF**₄ were characterized by multinuclear NMR (¹H, ¹³C, ³¹P) and IR spectroscopy and elemental analyses, including X-ray diffraction analysis of **1b**, **2**, and **3**.

Introduction

In the course of our studies with donor-substituted acetylenes^[1] we came across bis(amidinate) and bis(dithiocarboxylate) ligands, which show a direct linkage by acetylene moieties. Such acetylene-bis(amidinate) and acetylene-bis(dithiocarboxylate) ligands (**A**²⁻, **B**²⁻) as well as the mixed prototype **C**²⁻ (Figure 1) constitute interesting building blocks for one-dimensional coordination polymers. Within this scheme the individual donor moieties can either adopt a chelating or a bridging coordination mode. Homoleptic complexes with square-planar coordination structure, which could serve as linker, are well known for both amidinate^[2] and dithiocarboxylate^[3] ligands. In addition, the limited stability of complex centers with four-membered chelate rings is considered favorable for the formation of definite coordination polymers, because certain lability will allow the rearrangement of coordination misfits. The electronic cooperation of metal ions connected by the ligands **A**²⁻ to **C**²⁻ through the conjugated bridge might confer respective materials with desirable electronic properties like directed conductivity and high absorptivity at comparatively low energies. For instance, the Chisholm group presented recently dinuclear molybdenum and tungsten complexes, in which $M_2(\text{O}_2\text{CMe})_2$ units are coordinated by two phenylalkynyl- or ferrocenylalkynyl-amininate ligands in *trans*-configuration.^[4a] These complexes are highly colored and the ferro-

cene derivative shows electronic cooperation with the $M_2(\text{O}_2\text{CMe})_2$ moiety as indicated by cyclic voltammetry. Accordingly, related coordination polymers with **A**²⁻ represent promising materials with presumably interesting opto-electronic properties.

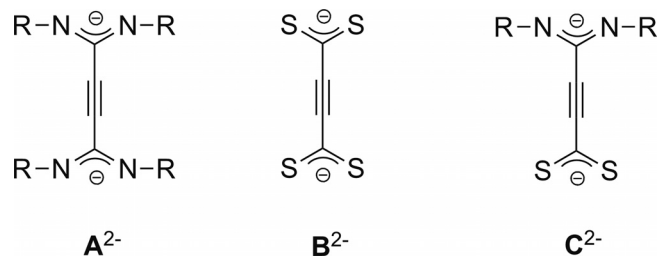


Figure 1. Amidinate- and dithiocarboxylate ligands bridged by an acetylene moiety.

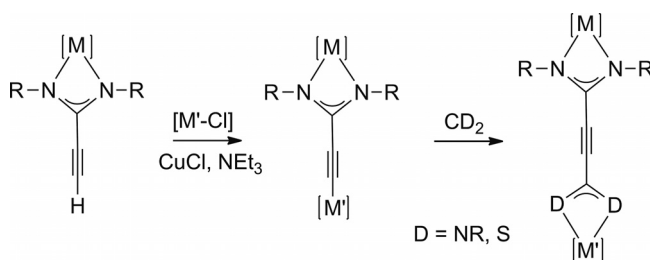
Whereas quite a number of coordination compounds of alkyne-amidinate ligands with predominantly lanthanide ions have appeared within the last years^[5] and some alkyne-dithiocarboxylate complexes were published within the last decades,^[6] complexes with ligands **A**²⁻ to **C**²⁻ are unknown so far. One reason for this gap seems to be the unclear access to the di-anionic ligands or, alternatively, the protonated forms. In preliminary attempts we encountered considerable difficulties in the synthesis of $\text{Li}_2\text{-A}$ and particularly $\text{Li}_2\text{-B}$. $\text{Li}_2\text{-A}$ ($R = \text{cyclo-C}_6\text{H}_{11}$) can be prepared by reaction of Li_2C_2 with dicyclohexylcarbodiimide in THF. After protonation the product $\text{H}_2\text{-A}$ was detected by mass spectrometry. However, the isolation of analytically pure samples by various purification methods turned out to be cumbersome due to the low solubility, which reflects the presumably polymeric structures. Accordingly, coordination experiments with the raw material $\text{Li}_2\text{-A}$

* Prof. Dr. W. W. Seidel
Fax: +49-381-4986382
E-Mail: wolfram.seidel@uni-rostock.de

[a] Universität Rostock
Institut für Chemie
Albert-Einstein-Straße 3a
18059 Rostock, Germany
[b] Westfälische Wilhelms-Universität Münster
Institut für Anorganische und Analytische Chemie
Corrensstraße 28/30
48149 Münster, Germany

led to equivocal products. Therefore, we sought for a step by step procedure for the generation of acetylene-bis(amidinate) ligands.

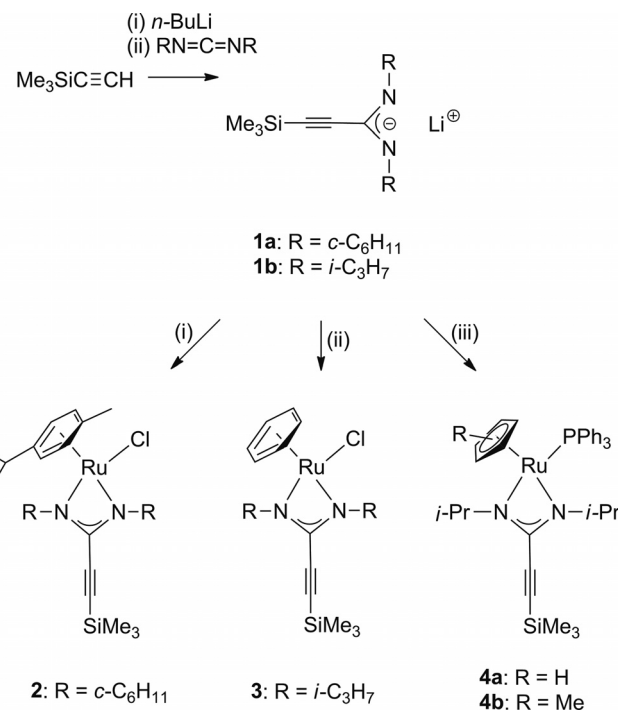
Our long-term approach comprises the synthesis of mononuclear complexes with hitherto unknown trimethylsilylethynylamidinate ligands and the subsequent insertion of a second amidinate or dithiocarboxylate group via the corresponding terminal alkyne after removal of the trimethylsilyl group. Insertions reactions of carbodiimides or CS₂ into metal-acetylide bonds according to Scheme 1 were regularly observed^[5d,5e,6a–c,6e] and respective catalytic procedures for the conversion of terminal alkynes into alkyne-amidinates are published.^[5a] In this contribution we give a progress report on the prospects of this strategy. We describe the synthesis and structure of trimethylsilylethynyl-amidinate ligands and a number of Ru^{II} complexes with ancillary π ligands. In addition, we report on investigations on the removal of the trimethylsilyl group in all complexes prepared.



Scheme 1. Outline of the synthetic strategy.

Results and Discussion

The lithium amidinates used for coordination experiments were prepared in ethyl ether from the reaction between either diisopropylcarbodiimide or dicyclohexylcarbodiimide and lithium trimethylsilylacetylide as shown in Scheme 2. The acetylide was obtained *in situ* by standard deprotonation of Me₃SiC≡CH, which is commercially available. The use of ethyl ether as solvent proved to be favorable, because Li[(*c*-C₆H₁₁N)₂CC≡CSiMe₃] (Li-1a) and Li[(*i*-C₃H₇N)₂CC≡CSiMe₃] (Li-1b) could be obtained in crystalline form as white salts. The solubility in THF is very high, whereas decomposition occurred in more polar and halogenated solvents. The compounds are very sensitive to hydrolysis and Li-1a being visibly more stable. Significant spectroscopic features are the ¹³C NMR shift of the alkyne carbon atoms at δ = 98.5 and 96.5 ppm (Li-1a). The low intensity of the latter signal is indicative of the carbon atom directly attached to the amidinate group. The amidinate carbon atom was detected at δ = 156.6 ppm for both Li-1a and Li-1b. Both samples were examined by single-crystal X-ray diffraction. The molecular structure of (Li-1b)₂·2Et₂O is depicted in Figure 2.



Scheme 2. Synthesis of alkynyl-amidinate ligands and its Ru^{II} complexes: (i) $[(\eta^6\text{-cymene})\text{RuCl}(\mu\text{-Cl})_2]$, THF; (ii) $[(\eta^6\text{-benzene})\text{RuCl}(\mu\text{-Cl})_2]$, THF; (iii) $[(\eta^5\text{-C}_5\text{R}_5)\text{Ru}(\text{PPh}_3)(\text{NCMe})_2]\text{PF}_6$ ($\text{R} = \text{H}, \text{Me}$), THF.

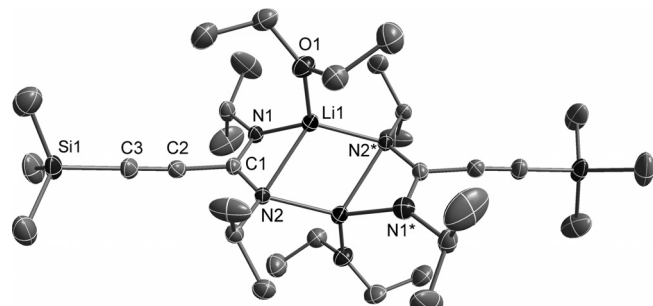


Figure 2. Molecular structure of dimer (Li-1b)₂·2Et₂O in the crystal with thermal ellipsoids set at 40% probability. Hydrogen atoms are omitted for clarity. Selected bond lengths /Å and angles /°: Li1–N1 2.002(4), Li1–N2 2.243(4), Li1–N2* 2.042(4), Li1–O1 1.923(4), C1–N1 1.324(3), C1–N2 1.331(3), C1–C2 1.466(3), C2–C3 1.203(3), C3–Si1 1.829(2), N1–C1–N2 119.8(2), C1–C2–C3 174.3(3), C2–C3–Si1 175.3(2).

Both examples form dimeric structures having a crystallographically imposed inversion center. The amidinate moieties serve as a chelate with one lithium ion, whereas one of the nitrogen donor atoms additionally bridges to the second lithium atom and vice versa. Accordingly, the lithium ions are four coordinate in a pseudo-tetrahedral fashion. This structural motif has been well documented and the metric parameters are not exceptional.^[4]

Metathesis reactions of the amidinate salts Li-1a and Li-1b with the Ru^{II} complexes $[(\eta^6\text{-cymene})\text{RuCl}(\mu\text{-Cl})_2]$ or $[(\eta^6\text{-benzene})\text{RuCl}(\mu\text{-Cl})_2]$ in THF led to the formation of the monomolecular complexes $[(\eta^6\text{-cymene})\text{RuCl}(1\mathbf{a})]$ and $[(\eta^6\text{-ben-$

zene)RuCl(**1b**)] according to Scheme 2. The neutral brown cymene and green benzene complexes are soluble in toluene and were eventually isolated analytically pure as [(η^6 -cymene)RuCl(**1a**)] (**2**) and [(η^6 -benzene)RuCl(**1b**)] (**3**) by crystallization from toluene solution at low temperature. The coordination of ruthenium alters the NMR spectroscopic features of the amidinate ligands only marginally. The ^{13}C NMR shift of the amidinate carbon atom is observed at 157.0 ppm for **2** and 156.2 ppm for **3**. Both complexes could be characterized by single-crystal X-ray diffraction. The molecular structure of **2** is depicted in Figure 3 together with relevant metrical parameters. The complex displays a standard half sandwich structure with η^6 -bonded cymene. The amidinate ligand **1a**⁻ is coordinated in a chelate like fashion to ruthenium. The remaining chloride substituent is directed almost perpendicular to the chelate ring plane spanned by N1, C1, N2, and Ru. The Ru–N bond lengths (Ru–N1 and Ru–N2) amount to 2.132(2) Å and 2.095(2) Å, respectively. The N1–C1–N2 angle has decreased to 111.2(2) $^\circ$ as compared with the corresponding angle of 119.8(2) $^\circ$ in Li-**1b**.

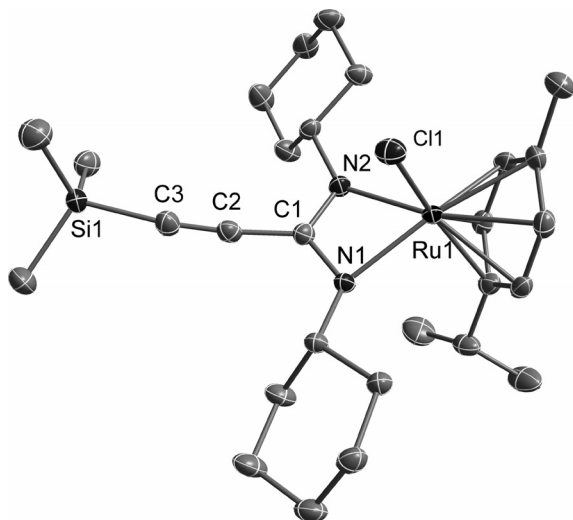


Figure 3. Molecular structure of **2** in the crystal with thermal ellipsoids set at 50% probability. Hydrogen atoms are omitted for clarity. Selected bond lengths /Å and angles /°: Ru1–N1 2.1318(17), Ru1–N2 2.0946(18), Ru1–Cl1 2.4213(6), C1–N1 1.327(3), C1–N2 1.320(3), C1–C2 1.448(3), C2–C3 1.198(3), C3–Si1 1.843(2), N1–C1–N2 111.2(2), C1–C2–C3 174.0(2), C2–C3–Si1 170.6(2).

The molecular structure of **3** is shown in Figure 4. The metrical parameters of the sterically less encumbered complex **3** are similar to that of **2**. The Ru–N distances of Ru–N1 with 2.088(2) Å and of Ru–N2 with 2.106(2) Å are somewhat but significantly shorter. The N1–C1–N2 angle amounts to 110.3(2) $^\circ$. The structure data are similar to related Ru^{II} amidinate complexes published by the Nagashima group,^[7] which show the weak influence of the type of π ligand at ruthenium and the substituent at the amidinate carbon atom on the Ru–N distance. However, steric effects are rather evident, because complex **2** shows a folding of the chelate ring about the NN axis of 18.3 $^\circ$ and a distinct deviation of the alkyne from linearity. Both features are much less pronounced in complex **3**.

Interestingly, the corresponding cationic 16-electron species [$(\eta^6\text{-C}_6\text{H}_6)_2\text{Ru}(i\text{PrN})_2\text{CMe}]^+$ displays a chelate ring folding of 31.4 $^\circ$, which is attributed to a weak π coordination of the amidinate.^[7a]

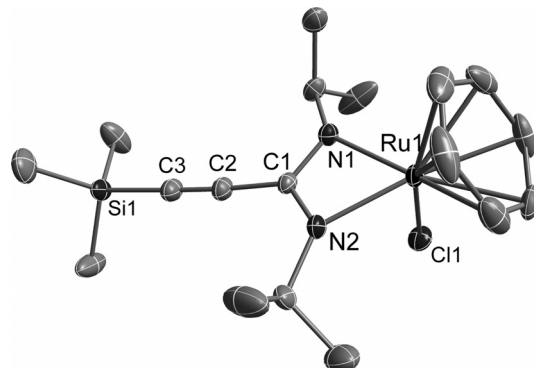
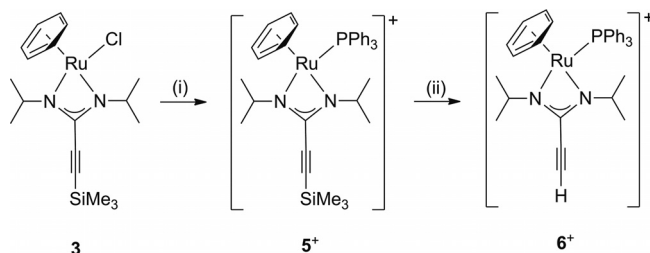


Figure 4. Molecular structure of **3** in the crystal with thermal ellipsoids set at 40% probability. Hydrogen atoms are omitted for clarity. Selected bond lengths /Å and angles /°: Ru1–N1 2.0878(18), Ru1–N2 2.1057(18), Ru1–Cl1 2.4083(7), C1–N1 1.322(3), C1–N2 1.321(3), C1–C2 1.448(3), C2–C3 1.198(3), C3–Si1 1.847(3), N1–C1–N2 110.3(2), C1–C2–C3 176.6(3), C2–C3–Si1 177.0(3).

Trimethylsilyl groups attached to alkyne carbon atoms are usually removed by fluoride ions in THF/methanol mixtures or with K_2CO_3 in methanol. Cleavage of the trimethylsilyl group is indeed observed with **2** and **3** as indicated by NMR spectroscopy; however, we were not able to isolate analytically pure products. We assume the persistent reactivity of the chloride substituent to be the reason for that observation. Therefore, we tried to substitute the chloride ion by neutral π -acceptor ligands like phosphanes and isocyanides in order to block that position. Reaction of the cymene complex **2** with $\text{Ag}[\text{BF}_4]$ in CH_2Cl_2 led to precipitation of AgCl , however, the coordination of different phosphanes or dimethylaminopyridine (DMAP) turned out to be impossible. Solely, adduct formation of the isocyanide *t*BuNC with intermediate [$(\text{cymene})\text{Ru}(\text{1a})$]⁺ could be proven spectroscopically (IR, NMR). We attribute this behavior to the strong steric hindrance in complex **2** as is evident in the molecular structure (Figure 3). Accordingly, reaction of the corresponding benzene complex **3** with $\text{Ag}[\text{BF}_4]$ in CH_2Cl_2 and subsequent addition of PPh_3 resulted smoothly in the formation of the reddish brown phosphane complex [$(\eta^6\text{-benzene})\text{Ru}(\text{1b})(\text{PPh}_3)$] BF_4 (**5** \cdot BF_4) (Scheme 3). The air-stable complex, which could be isolated by precipitation from a THF/*n*-hexane solvent mixture, was characterized spectroscopically. The ^{31}P NMR shift of **5** \cdot BF_4 was found at 33.1 ppm; the amidinate carbon atom resonates at 163.7 ppm in the ^{13}C NMR spectrum. The identity of **5** \cdot BF_4 is further substantiated by elemental analysis and MALDI-TOF mass spectrometry. Subsequent reaction of **5** \cdot BF_4 with catalytic amounts of $[\text{Bu}_4\text{N}]^+$ in THF/ CH_3OH yielded slowly the complex [$(\eta^6\text{-C}_6\text{H}_6)_2\text{Ru}(i\text{PrN})_2\text{CC}\equiv\text{CH}(\text{PPh}_3)$] BF_4 (**6** \cdot BF_4) with a terminal alkyne function. The ^{31}P NMR resonance of complex **6** \cdot BF_4 was detected to be only slightly changed at 32.9 ppm. The most dramatic shift observed in the ^{13}C NMR spectra going from **5** \cdot BF_4 to **6** \cdot BF_4 applies to the alkyne carbon atom attached to

silicon in **5**-BF₄ (96.4 ppm) and to hydrogen in **6**-BF₄ (67.8 ppm). The range around 70 ppm is typical for terminal protons of alkynes. In addition, the cation [**6**⁺] (*m/z* = 593) could be identified by MALDI-TOF mass spectrometry.



Scheme 3. Synthesis of a Ru^{II} ethynylamidinate complex: (i) Ag[BF₄], PPh₃, CH₂Cl₂; (ii) [Bu₄N]F, MeOH, THF.

In order to test the influence of the total charge on the reproducibility and complex stability we additionally synthesized the complexes [(η⁵-C₅H₅)Ru(PPh₃)(**1b**)] (**4a**) and [(η⁵-C₅Me₅)Ru(PPh₃)(**1b**)] (**4b**). Both were accessible by reaction of Li-**1b** with the acetonitrile complexes [(η⁵-C₅R₅)Ru(PPh₃)(NCMe)₂]PF₆ (*R* = H, Me) according to Scheme 2. The neutral complexes **4a** and **4b**, which were isolated from toluene solution, show ³¹P NMR resonances at 46.9 and 46.1 ppm, respectively. The reaction of **4a/b** with a catalytic quantity of [Bu₄N]F in THF/CH₃OH led to the removal of the trimethylsilyl group as indicated by ¹H NMR evidence. The crude product [(η⁵-C₅H₅)Ru{(iPrN)₂CC≡CH}(PPh₃)] (**7**) displayed a ³¹P NMR resonance at 51.8 ppm and the correct molecular mass of *m/z* = 580 in the MALDI-TOF mass spectrum. However, we were not able to isolate an analytically pure sample of complex **7**. The corresponding reaction with **4b** led to an even more intricate reaction mixture.

Conclusions

The coordination of trimethylsilylethynyl-amidinate ligands at Ru^{II} half sandwich complexes (*R* = cymene, benzene, cyclopentadienyl) could be readily achieved by salt metathesis. Beforehand, the respective Li-amidinate ligands were straightforwardly obtained by deprotonation of trimethylsilylacetylene and subsequent reaction with carbodiimides (*R* = cyclohexyl, isopropyl). The intended removal of the trimethylsilyl group at the complexes was observed in all cases. However, the isolation of stable and pure ethynylamidinate complexes turned out to be very sensitive to the particular ligand set. Ambiguous conversions were particularly observed with chlorido substituents at ruthenium. Best results were obtained with cationic [(η⁶-C₆H₆)Ru(**1b**)(PPh₃)]BF₄ leading to the desired complex [(η⁶-C₆H₆)Ru{(iPrN)₂CC≡CH}(PPh₃)]BF₄. We assume that consecutive reactions with the terminal alkyne proton like formation of vinylidene complexes, which is typical for Ru^{II}, could explain the restricted applicability of the approach with Ru^{II}. Further investigations with more Lewis acidic and less electron rich metal ions are underway.

Experimental Section

General: All operations were carried out in a dry argon atmosphere by using standard Schlenk and glove box techniques. All solvents were dried and saturated with argon by standard methods and freshly distilled prior to use. Trimethylsilylacetylene was purchased from Aldrich. [(η⁶-cymene)RuCl(μ-Cl)]₂, [(η⁶-benzene)RuCl(μ-Cl)]₂, [(η⁵-C₅H₅)Ru(PPh₃)(NCMe)₂]PF₆, and [(η⁵-C₅Me₅)Ru(PPh₃)(NCMe)₂]PF₆ were synthesized according to literature procedures.^[8] NMR spectra (¹H, ³¹P, ¹³C) were recorded with the Bruker spectrometers AC 200 and Avance 400. Elemental analyses were performed with a Vario EL III CHNS elemental analyzer. MALDI mass spectra were obtained with a Bruker Reflex IV spectrometer using [(2E)-3-(4-*tert*-butylphenyl)-2-methylprop-2-enyliden]malononitrile (DCTB) as matrix. Infrared spectra were recorded with a Bruker Vektor 22 spectrometer.

Li[(c-C₆H₁₁N)₂CC≡CSiMe₃] (Li-1a): Trimethylsilylacetylene (4.3 mL, 30 mmol) dissolved in diethyl ether (40 mL) and cooled to -78 °C was treated with *n*-butyllithium (2.5 M solution in *n*-hexane, 12 mL). After 10 min 1,3-dicyclohexyl-carbodiimide (6.2 g, 30 mmol) was added and the mixture was stirred for 30 min at -78 °C. Upon warming to room temperature, the reaction was complete in the course of two h. Then the solution was concentrated to a small volume and cooled to -30 °C overnight. The precipitate formed was filtered off, washed with cold diethyl ether (3 mL) and dried in vacuo. The product was recrystallized from diethyl ether/*n*-hexane (5:1). Yield 91 %. Elemental analysis C₂₂H₄₁LiN₂Osi (384.60 g·mol⁻¹): C 69.05 (calcd. 68.70); H 10.66 (10.75); N 7.42 (7.28)%. ¹H NMR (200 MHz, [D₈]THF, 25 °C): δ = 3.42 (m, 2 H, CH), 1.75–1.00 (m, 20 H, CH₂), 0.18 (s, 9 H, SiCH₃) ppm. ¹³C NMR (50 MHz, [D₈]THF, 25 °C): δ = 156.6 (CN), 98.5 (SiC≡C), 96.5 (CC≡C), 59.0 (CH), 38.0 (CHCH₂), 27.3 (CHCH₂CH₂), 27.0 (CHCH₂CH₂CH₂), 0.2 (SiCH₃) ppm. IR (KBr): ν 2144 (s, C≡C), 1597 (s, CN) cm⁻¹. MS (MALDI): *m/z* = 305 (M⁺ + 2 H, 100 %).

Li[(iPrN)₂CC≡CSiMe₃] (Li-1b): Li-1b was prepared in a scale of 50 mmol (50 mL diethyl ether) as described for Li-1a by using 1,3-diisopropylcarbodiimide (6.9 mL, 50 mmol). Yield 76 %. Elemental analysis C₁₆H₃₃LiN₂Osi (304.47 g·mol⁻¹): C 62.42 (calcd. 63.12), H 10.81 (10.92), N 9.38 (9.20)%. ¹H NMR (200 MHz, [D₈]THF, 25 °C): δ = 3.78 (sept, ³J = 6.2 Hz, 2 H, CH), 0.97 [d, ³J = 6.2 Hz, 12 H, CH(CH₃)₂], 0.17 (s, 9 H, SiCH₃) ppm. ¹³C NMR (50 MHz, [D₈]THF, 25 °C): δ = 156.6 (CN), 98.0 (SiC≡C), 97.1 (CC≡C), 50.1 [CH(CH₃)₂], 26.8 [CH(CH₃)₂], 0.2 (SiCH₃) ppm. IR (KBr): ν 2137 (s, C≡C), 1605 (s, CN) cm⁻¹. MS (MALDI): *m/z* = 225 (M⁺ + 2 H, 100 %).

[(η⁶-Cymene)RuCl(1a)] (2): A solution of Li-1a (675 mg, 2.17 mmol) in THF (20 mL) was added to a suspension of [(η⁶-cymene)RuCl(μ-Cl)]₂ (604 mg, 1.09 mmol) in THF (70 mL). After stirring overnight, the solvent was evaporated under reduced pressure. The residue was extracted into toluene (3 × 10 mL), filtered and the solvent was evaporated to dryness. Yield 99 %. Complex **2** crystallized in analytically pure form from a saturated toluene solution upon cooling to -30 °C. Elemental analysis C₂₈H₄₅CIN₂RuSi (574.28 g·mol⁻¹): C 59.02 (calcd. 58.56), H 7.98 (7.90), N 4.79 (4.88)%. ¹H NMR (400 MHz, CDCl₃, 25 °C): δ = 5.03 [d, ³J = 6.4 Hz, 2 H, (CH₃)₂-CHCCH], 4.74 (d, ³J = 6.4 Hz, 2 H, CH₃CCH), 3.49 (m, 2 H, NCH), 2.65 (sept, ³J = 6.8 Hz, 1 H, CCH), 2.43 (m, 2 H, CHCH₂), 2.25 (m, 2 H, CHCH₂), 2.05 (s, 3 H, CCH₃), 1.85–1.20 [m, 16 H, NCH(CH₂)₂-(CH₂)₂CH₂], 1.09 [d, ³J = 6.8 Hz, 6 H, CH(CH₃)₂], 0.05 (s, 9 H, SiCH₃) ppm. ¹³C NMR (100 MHz, CDCl₃, 25 °C): δ = 157.0 (CN), 99.3 [CCH(CH₃)₂], 98.6 (CCH₃), 97.0 (SiC≡C), 94.7 (CC≡C), 79.7, 78.5 (Ar-C), 58.9 (NCH), 36.9, 36.2 [NCH(CH₂)₂], 32.4 [CCH(CH₃)₂], 26.7, 26.4, 26.3 [NCH(CH₂)₂(CH₂)₂CH₂], 22.8 [CCH(CH₃)₂], 19.4

(CCH₃), -0.4 (SiCH₃) ppm. **MS** (MALDI): *m/z* = 574 (M⁺, 30%); 539 (M⁺-Cl, 100%).

[(η⁶-Benzene)RuCl(1b)] (3): A solution of compound Li-**1b** (461 mg, 2.00 mmol) in THF (20 mL) was added to a suspension of [(η⁶-benzene)RuCl(μ-Cl)]₂ (1.00 g, 2.00 mmol) in THF (50 mL). After stirring overnight, the solvent was evaporated under reduced pressure. The residue was extracted into toluene (3 × 10 mL), filtered and the green filtrate was reduced in volume. Complex **3** crystallized upon cooling to -30 °C. Yield 81%. Elemental analysis C₁₈H₂₉ClN₂RuSi (438.05 g·mol⁻¹): C 49.96 (calcd. 49.35), H 6.78 (6.67), N 6.28 (6.40) %. **¹H NMR** (200 MHz, C₆D₆, 25 °C): δ = 4.93 (s, 6 H, η⁶-C₆H₆), 3.99 (sept, ³J = 6.2 Hz, 2 H, CH), 1.43 (d, ³J = 6.2 Hz, 6 H, CH₃), 1.31 (d, ³J = 6.2 Hz, 6 H, CH₃), 0.06 (s, 9 H, SiCH₃) ppm. **¹³C NMR** (50 MHz, C₆D₆, 25 °C): δ = 156.2 (CN), 97.1 (SiC≡C), 93.8 (CC≡C), 81.3 (η⁶-C₆H₆), 50.6 [CH(CH₃)₂], 25.6, 25.5 [CH(CH₃)₂], -0.5 (SiCH₃) ppm. **MS** (MALDI): *m/z* = 438 (M⁺, 80%); 403 (M⁺-Cl, 100%).

[(η⁵-C₅H₅)Ru(1b)(PPh₃)] (4a): A solution of Li-**1b** (78 mg, 0.34 mmol) in THF (20 mL) was added to a solution of [(η⁵-C₅H₅)Ru(PPh₃)(NCMe)₂]PF₆ (300 mg, 0.34 mmol) in THF (40 mL). After stirring overnight, the solvent was evaporated under reduced pressure. The residue was extracted into toluene (3 × 10 mL) and filtered. Concentration and cooling to -30 °C yielded the product as a brown solid. Yield 72%. **¹H NMR** (200 MHz, C₆D₆, 25 °C): δ = 7.20–7.00 (m, Ar-H), 4.33 (s, η⁵-C₅H₅), 3.82 (sept, ³J = 6.4 Hz, 2 H, CH), 1.21 [d, ³J = 6.4 Hz, 6 H, CH(CH₃)₂], 0.64 [d, ³J = 6.4 Hz, 6 H, CH(CH₃)₂], 0.16 (s, 9 H, SiCH₃) ppm. **³¹P NMR** (81 MHz, C₆D₆, 25 °C): δ = 46.9 (PPh₃) ppm. **MS** (MALDI): *m/z* = 429 (M⁺-**1b**, 40%).

[(η⁵-C₅Me₅)Ru(1b)(PPh₃)] (4b): Compound **4b** was prepared as described for **4a**. **¹H NMR** (200 MHz, C₆D₆, 25 °C): δ = 7.40–6.80 (m, Ar-H), 3.39 (sept, ³J = 6.4 Hz, 2 H, CH), 2.11 [s, η⁵-C₅(CH₃)₅], 1.25 [d, ³J = 6.4 Hz, 6 H, CH(CH₃)₂], 1.21 [d, ³J = 6.4 Hz, 6 H, CH(CH₃)₂], 0.14 (s, 9 H, SiCH₃) ppm. **³¹P NMR** (81 MHz, C₆D₆, 25 °C): δ = 46.1 (PPh₃) ppm. **MS** (MALDI): *m/z* = 499 (M⁺-**1b**, 40%).

[(η⁶-C₆H₆)Ru(1b)(PPh₃)]BF₄ (5-BF₄): A solution of **3** (1.00 g, 1.91 mmol) in dichloromethane (50 mL) was cooled to -78 °C. AgBF₄ (372 mg, 1.91 mmol) was added. The resulting mixture was warmed to room temperature and stirred for 30 min. To the resulting brown suspension PPh₃ (600 mg, 1.91 mmol) was added. The mixture was stirred for 2 h and then dried by evaporation of the volatiles. The residue was dissolved in THF, filtered, and the filtrate was reduced to a small volume. The addition of hexane followed by cooling afforded the product as a brown solid. Yield 71%. Elemental analysis C₃₆H₄₄BF₄N₂PRuSi (751.68 g·mol⁻¹): C 58.02 (calcd. 57.52), H 5.95 (5.90), N 3.69 (3.73) %. **¹H NMR** (200 MHz, CDCl₃, 25 °C): δ = 7.48–7.20 (m, 15 H, Ar-H), 5.77 (s, 6 H, η⁶-C₆H₆), 3.25 [sept, ³J = 6.2 Hz, 2 H, CH(CH₃)₂], 0.97 (d, ³J = 6.2 Hz, 6 H, CH₃), 0.81 (d, ³J = 6.2 Hz, 6 H, CH₃), 0.19 (s, 9 H, SiCH₃) ppm. **¹³C NMR** (50 MHz, CDCl₃, 25 °C): δ = 163.7 (CN), 134.3–128.4 (Ar-C), 96.4 (SiC≡C), 92.2 (CC≡C), 89.1 (η⁶-C₆H₆), 51.2 [CH(CH₃)₂], 24.0, 23.3 [CH(CH₃)₂], -0.8 (SiCH₃) ppm. **³¹P NMR** (81 MHz, CDCl₃, 25 °C): δ = 33.08 (PPh₃) ppm. **MS** (MALDI): *m/z* = 665 (M⁺, 100%), 403 (M⁺-PPh₃, 30%).

[(η⁶-C₆H₆)Ru{(iPrN)₂CC≡CH}(PPh₃)]BF₄ (6-BF₄): Pure **5-BF₄** (217 mg, 0.30 mmol) was dissolved in THF (15 mL). Methanol (8 mL) and tetrabutylammonium fluoride (7 mg, 0.02 mmol) were added and the mixture was stirred for 3 d at room temperature. After removal of the solvents under reduced pressure **6-BF₄** was obtained from THF/n-hexane and cooling to -40 °C as a brown solid. Yield 91%. Elemental analysis C₃₃H₃₆BF₄N₂PRu (679.50 g·mol⁻¹): C 58.92 (calcd. 58.33), H 5.39 (5.34), N 4.05 (4.12) %. **¹H NMR** (200 MHz, CDCl₃, 25 °C): δ = 7.71–7.26 (m, 15 H, Ar-H), 5.77 (s, 6 H, η⁶-C₆H₆), 3.16 [m, 2 H, CH(CH₃)₂], 2.14 (C≡CH), 0.98, 0.90 (m, 12 H, CHCH₃) ppm. **¹³C NMR** (50 MHz, CDCl₃, 25 °C): δ = 155.3 (CN), 134.1–127.9 (Ar-C), 89.1 (η⁶-C₆H₆), 88.5 (CC≡C), 67.8 (HC≡C), 57.0 [CH(CH₃)₂], 24.2, 23.3 [CH(CH₃)₂] ppm. **³¹P NMR** (81 MHz, CDCl₃, 25 °C): δ = 32.9 (PPh₃) ppm. **MS** (MALDI): *m/z* = 593 (M⁺, 100%); 331 (M⁺-PPh₃, 80%).

Table 1. Crystallographic details for Li-**1b**, **2** and **3**.

	(Li- 1b) ₂ ·2Et ₂ O	2	3
Formula	C ₃₂ H ₆₆ Li ₂ N ₄ O ₂ Si ₂	C ₂₈ H ₄₅ ClN ₂ RuSi	C ₁₈ H ₂₉ ClN ₂ RuSi
M _w /g·mol ⁻¹	608.95	574.27	438.04
Color / Habit	colorless, plates	orange, prisms	brown, prisms
Crystal system	triclinic	monoclinic	monoclinic
Space group	P̄1	P ₂ 1/n	P ₂ 1/c
a /Å	9.4334(19)	10.9689(13)	11.7906(16)
b /Å	9.908(2)	8.7138(10)	15.920(2)
c /Å	13.285(3)	30.480(4)	12.0483(16)
a /°	68.274(4)	90	90
β /°	82.780(4)	90.035(2)	114.246(2)
γ /°	62.056(4)	90	90
V /Å ³	1017.3(4)	2913.3(6)	2062.0(5)
Z	1	4	4
D _{calcd.} /g·cm ⁻³	0.994	1.309	1.411
μ /mm ⁻¹	0.116	0.689	0.949
T /K	153	153	153
2θ _{max} /°	47.0	60.1	60.06
Collected refl.	7183	32383	23590
Unique refl. / R _{int}	3003 / 0.0280	8480 / 0.0424	6016 / 0.0475
Variables	199	304	215
R ₁ [[I > 2σ(I)]]	0.0500	0.0415	0.0363
wR ₂ (all data)	0.1437	0.0827	0.0843
GooF on F ²	0.894	1.122	1.036
Res.dens. /e·Å ⁻³	0.524 / -0.302	0.819 / -0.735	0.801 / -0.386

[($\eta^5\text{-C}_5\text{H}_5$)Ru{(iPrN)₂CC≡CH}(PPh₃)] (7): Complex **7** was obtained following the same procedure as described for **6**-BF₄, using **4a** instead of **5**-BF₄. Yield 95%. **¹H NMR** (200 MHz, C₆D₆, 25 °C): δ = 7.20–6.90 (m, Ar-H), 4.46 (s, C₅H₅), 3.40 (m, 2 H, CH), 2.11 (s, 1H, C≡CH), 1.20 [d, ³J = 6.0 Hz, 6 H, CH(CH₃)₂], 0.75 [d, ³J = 6.0 Hz, 6 H, CH(CH₃)₂] ppm. **³¹P NMR** (81 MHz, C₆D₆, 25 °C): δ = 51.8 (PPh₃) ppm. **MS** (MALDI): *m/z* = 580 (M⁺, 30%); 429 {M⁺–[(iPrN)₂CC≡CH]}, 10%.

Crystal Structure Determination: Single crystals suitable for X-ray diffraction analysis were coated with a perfluoropolyether, picked up with a glass fiber and immediately mounted in the cold nitrogen stream of the diffractometer. Intensity data were collected at *T* = 153 K with a Bruker AXS Apex CCD diffractometer equipped with a rotating anode using graphite monochromated Mo-K_α radiation. Data collection, cell refinement, data reduction and integration as well as absorption correction were performed with the Bruker AXS program packages SMART, SAINT and SADABS. Structure solutions were found with SHELXS^[9a] by direct methods and were refined with SHELXL^[9b] against *F*_o² by using anisotropic thermal parameters for all non-hydrogen atoms. Hydrogen atoms were included at calculated positions with fixed thermal parameters. A summary of the crystallographic data and structure refinement results for complexes [(Li-**1b**), **2**, and **3** are given in Table 1.

1b)₂·2Et₂O], CCDC-845855 (**2**), and CCDC-845856 (**3**) (Fax: +44-1223-336-033; E-Mail: deposit@ccdc.cam.ac.uk, http://www.ccdc.cam.ac.uk).

Acknowledgement

W. W. S. thanks Prof. F. E. Hahn for generous support.

References

- [1] a) W. W. Seidel, M. D. Ibarra Arias, M. Schaffrath, K. Bergander, *Dalton Trans.* **2004**, 2053–2054; b) W. W. Seidel, M. Schaffrath, T. Pape, *Chem. Commun.* **2006**, 3999–4000; c) W. W. Seidel, M. J. Meel, U. Radius, M. Schaffrath, T. Pape, *Inorg. Chem.* **2007**, 46, 9616–9629; d) W. W. Seidel, B. Lopez Sanchez, M. Meel, A. Hepp, T. Pape, *Eur. J. Inorg. Chem.* **2007**, 936–943; e) W. W. Seidel, M. J. Meel, F. Hupka, J. J. Weigand, *Dalton Trans.* **2010**, 39, 624–631.
- [2] a) D. A. Kissounko, M. V. Zabalov, G. P. Brusova, D. A. Lemenovskii, *Russ. Chem. Rev.* **2006**, 75, 351–374; b) F. T. Edelmann, *Chem. Soc. Rev.* **2009**, 38, 2253–2268; c) C. Jones, *Coord. Chem. Rev.* **2010**, 254, 1273–1289.
- [3] a) C. Bellitto, *Comments Inorg. Chem.* **1988**, 8, 101–124; b) N. Kano, T. Kawashima, *Top. Curr. Chem.* **2005**, 251, 141–180.
- [4] a) D. J. Brown, M. H. Chisholm, J. C. Gallucci, *Dalton Trans.* **2008**, 1615–1624; b) P. C. Junk, M. L. Cole, *Chem. Commun.* **2007**, 1579–1590.
- [5] a) W.-X. Zhang, M. Nishiura, Z. Hou, *J. Am. Chem. Soc.* **2005**, 127, 16788–16789; b) A. G. M. Barrett, M. R. Crimmin, M. S. Hill, P. B. Hitchcock, S. L. Lomas, M. F. Mahon, P. A. Procopiou, K. Suntharalingam, *Organometallics* **2008**, 27, 6300–6306; c) C. N. Rowley, T.-G. Ong, J. Priem, D. S. Richeson, T. K. Woo, *Inorg. Chem.* **2008**, 47, 12024–12031; d) W. J. Evans, J. R. Walen-sky, J. W. Ziller, A. L. Rheingold, *Organometallics* **2009**, 28, 3350–3357; e) M. L. Cole, G. B. Deacon, C. M. Forsyth, P. C. Junk, D. Polo-Ceron, J. Wang, *Dalton Trans.* **2010**, 39, 6732–6738; f) P. Droese, C. G. Hrib, F. T. Edelmann, *J. Organomet. Chem.* **2010**, 695, 1953–1956.
- [6] a) M. I. Bruce, M. J. Liddell, M. R. Snow, E. R. T. Tiekkink, *J. Organomet. Chem.* **1988**, 352, 199–204; b) V. Cadierno, M. P. Gamasa, J. Gimeno, E. Lastra, *J. Organomet. Chem.* **1996**, 510, 207–211; c) M. I. Bruce, B. C. Hall, N. N. Zaitseva, B. W. Skelton, A. H. White, *J. Chem. Soc. Dalton Trans.* **1998**, 1793–1804; d) H. M. Adams, P. E. Morris, M. J. Spey, S. E. Wright, *J. Organomet. Chem.* **2001**, 619, 209–217; e) P. Mathur, A. K. Ghosh, S. Mukhopadhyay, C. Srinivasu, S. M. Mobin, *J. Organomet. Chem.* **2003**, 678, 142–147; f) M. El-khatib, H. Goerls, W. Weigand, *J. Organomet. Chem.* **2006**, 691, 2055–2059.
- [7] a) T. Hayashida, Y. Yamaguchi, K. Kirchner, H. Nagashima, *Chem. Lett.* **2001**, 954–955; b) T. Hayashida, H. Nagashima, *Organometallics* **2002**, 21, 3884–3888; c) T. Hayashida, H. Kondo, J. Terasawa, K. Kirchner, Y. Sunada, H. Nagashima, *J. Organomet. Chem.* **2007**, 692, 382–394.
- [8] a) M. A. Bennett, A. K. Smith, *J. Chem. Soc. Dalton Trans.* **1974**, 233–241; b) E. Rüba, W. Simanko, K. Mauthner, K. M. Soldouzi, C. Slugovc, K. Mereiter, R. Schmid, K. Kirchner, *Organometallics* **1999**, 18, 3843–3850; c) M. I. Bruce, R. C. Wallis, *Aust. J. Chem.* **1979**, 32, 1471–1485.
- [9] a) G. M. Sheldrick, *Acta Crystallogr., Sect. A* **1990**, 46, 467–473; b) G. M. Sheldrick, *Acta Crystallogr., Sect. A* **2008**, 64, 112–122.

Received: September 27, 2011

Published Online: November 29, 2011